Investigations of core level states in epitaxial grown Si layers by electron energy loss spectrometry

M Stöger, C Hébert, E C Karl-Rückert, P Schattschneider, B Rau[1], S Gall[1] and H W Zandbergen[2]

Institute for Solid State Physics, Vienna University of Technology, A-1040 Vienna/Austria
[1] Hahn-Meitner-Institut Berlin, SE1 – Silizium Photovoltaik, D-12489 Berlin, Germany
[2] National Centre for High Resolution Microscopy, TU Delft, NL-2628 Delft, The Netherlands

ABSTRACT: Electron energy loss spectrometry (EELS) studies were carried out on epitaxially grown Si thin films which were deposited at low temperatures on Si (100) substrates by electron cyclotron resonance chemical vapour deposition (ECR CVD). The films were grown as a first step in order to realise crystalline thin film Si solar cells on foreign substrates. By means of electron diffraction in a transmission electron microscope (TEM) local polycrystalline defects in the films were investigated. EELS was used to analyse changes of bond length as a function of core level shifts. Comparisons with simulations of the WIEN2k code are presented.

1. INTRODUCTION

Using transmission electron microscopes with high energy resolved sources like cold field emitter electron guns or conventional field emitters with a pre-specimen monochromator resolutions in EEL spectra of less than 0.2eV can easily be reached. With such set-ups small core level shifts are observed at grain boundaries. The core level shifts can be led back to a change in bond length which introduces a shift in the density of unoccupied states of the boundary forming atoms. The role of core level shifts has often been ignored in EELS even though small changes in bond length can lead to large core level shifts (Muller 1999). This is probably due to the popular interpretation of core level shifts resulting from charge transfers. However the charge transfer interpretation is highly problematic for metals and semiconductors (Steiner 1981), and is known to fail in X-ray photoelectron spectroscopy (XPS). A more direct connection between core level shifts and bonding changes in metals already exists and has long been used for explaining the origins of surface-core level shifts in XPS (Citrin et al 1978, 1983 and Eastman et al 1982).

In the present work shifts of the ionisation edge threshold energy in EEL spectra of microtwins and polycrystalline defects in an epitaxial grown Si thin film are investigated. The shifts can be led back to a dilation of bonding because other effects on the EEL spectrum like impurities could be excluded. A crystallographic analysis of the defects was performed and high resolution TEM (HRTEM) images give insights into the dimension of the microtwins and defects.

Augmented plane wave calculations were performed using the WIEN2k code (Blaha 2002) to quantify the changes of bond length. This quantification is in good agreement with HRTEM measurements.

2. EXPERIMENTAL

The crystalline silicon (c-Si) thin film (d~2230nm) was deposited by ECR CVD. But epitaxial growth often is accompanied by defect formation. Usually polycrystalline (pc) defects can be observed (Mizushima 1999), sometimes amorphous cones are reported (i.e. Platen 2001). For TEM and EELS investigations plan view samples and cross section specimen were prepared by grinding

and ion milling. The last step of ion milling was done under low voltage conditions (~1kV) to remove beam damage from earlier preparation steps. After preparation the specimens were transferred to the microscope in a vacuum box to protect against oxidation.
High resolution microscopy and electron diffraction were done with an TECNAI F20 ST. EELS measurements were realised in the TECNAI F200 mono of TU Delft which is equipped with a pre-specimen Wien-type monochromator, an ultra stable high tension tank and an high resolution spectrometer. With this set-up energy resolution of EELS spectra of 0.12eV full width at half maximum (FWHM) in the zero loss peak (ZLP) can be reached without undue effort. The spectrometer dispersion was set to 0.02eV per channel for band gap measurements and 0.2eV for core level measurements. All EELS measurements were done in nanoprobe mode of the microscope that allows spot sizes down to 3Å. For our experiments we chose a spot size of 8Å to have more intensity in the EEL signal.

3. CRYSTALLOGRAPHY

3.1 Defect Orientations

In plan view projection all polycrystalline defects have a squared shape and consist of needle-like crystals. In figure 1 the shadow image shows that the orientation of the matrix is (100). The borders of the defects in the shadow image are perpendicular to the (220) diffraction spot, therefore the squared shape of the defect are in (110) orientation respectively to the matrix. This is also the preferred direction for microtwinning, as shown in section 3.2. Moreover, nearly all defects can be identified to

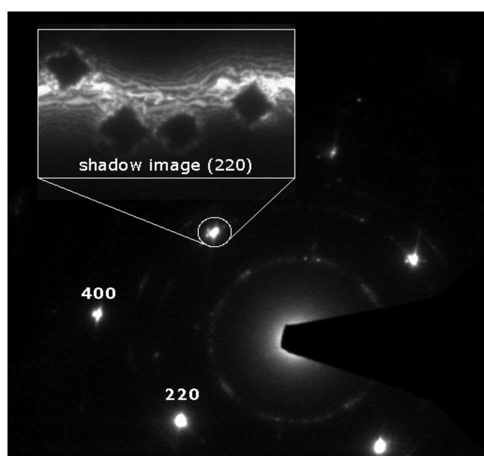

Figure 1: Diffractogramme of the matrix. The inlay shows a shadow image in plan view projection. The borders of the defects are all perpendicular to the (220) diffraction spot. (The (110) diffraction spot is not visible in the diffraction image, because it is a forbidden one.)

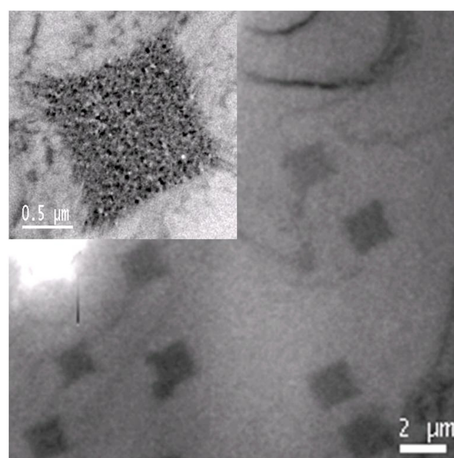

Figure 2: Plan view TEM image some defects. Most defects have the same size. The inlet proves that the defects have a polycrystalline structure, which was verified by electron diffraction, too. The scale bar of the inlet is 0.5µm.

have the same size (figure 2). This leads to the conclusion that most defects start to grow at the interface. A typical representative of this species is shown in figure 3c. The polycrystalline structure is clearly visible. The needles are perpendicular to the thin film-substrate interface. At the edges of the defect lines with an angle of 35.4° to the surface normal can be identified which is the (111) direction. These lines are identified as the microtwins that are shown in detail in figure 3d. A small impurity like a lattice defect of the substrate of an atom of a foreign species can be the reason. On the other hand the epitaxial growth seem to work well in the ECR CVD reactor, because only a view smaller defects were observed which may start to grow somewhere inside the thin film.

3.2 Microtwinning – Orientations and Sizes

In figure 3 electron diffraction images of the matrix from the left (a) and right (b) hand side of a defect (c) are shown. The typical features for microtwinning like the additional diffraction spots at each third of the distance and the streaks connecting the diffraction spots are clearly visible. An high-resolution acquisition (d) shows the microtwins on the right hand side of the defect (marked with *B* in image c). The microtwins have a thickness of 3-5 monolayers and are oriented in the (111) planes of the matrix.

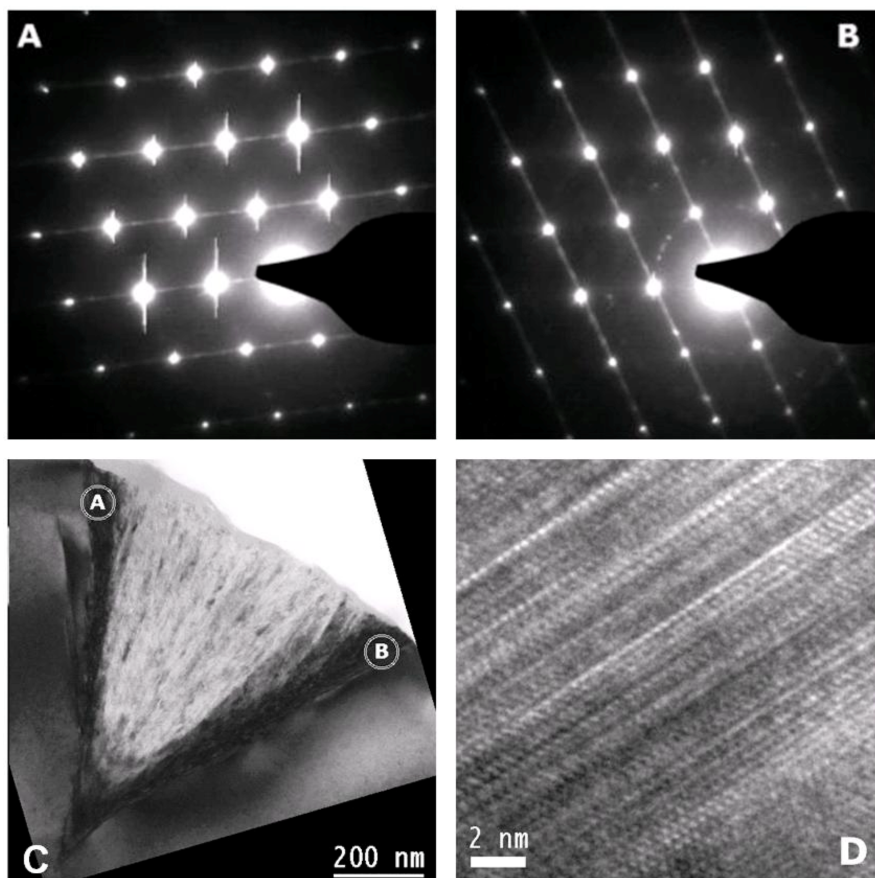

Figure 3: Diffraction pattern acquired at the left (A) and right (B) hand side of the defect shown in (C). The high resolution TEM image (D) shows that the microtwins have a thickness of only 3-5 monolayers and are oriented in (111) direction.

4. CORE LEVEL SHIFTS

EELS measurements were done at the cross sectional prepared specimen in three different positions. In figure 5 the second derivative of the Si-$L_{2,3}$ edge is shown to improve visibility of the energy shifts. Spectrum *c-Si* was acquired in a crystalline perfect region of the layer whereas *pc-Si* and *microtwins* were collected in the defect and the twinned region, respectively. The shift between *c-Si* and *pc-Si* is 0.2eV and *microtwins* is shifted by +0.3eV. Another possible effect that might be responsible for the shifts are band gap changes and was investigated, too. Direct measurements of the Si band gap in EELS were not successful because changes in the range of 0.1eV can hardly be observed but are predicted by simulations (figure 6). Augmented plane waves calculations were used to simulate the energy shift of the edge onset of the Si $L_{2,3}$, L_1, and K edge (figure 6). Due to the fact that the edge onset energy depends on the band gap and the total energy of the electrons the band gap energy was

calculated which is varying with bond length by about ±0.1eV for a change of ±2% in the lattice parameter. The energy shifts correspond to dilation in bond length of 1.86% and 2.48%.

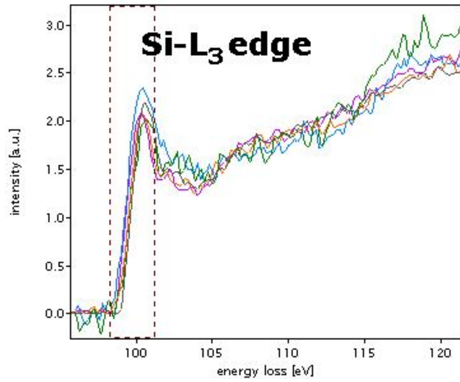

Figure 4: Si-L_3 edge at 99 eV energy loss. The 2nd derivative of the edge up to 109eV is shown more detailed in fig. 5. In the region of interest it is clearly visible that the edge onsets are at different energies.

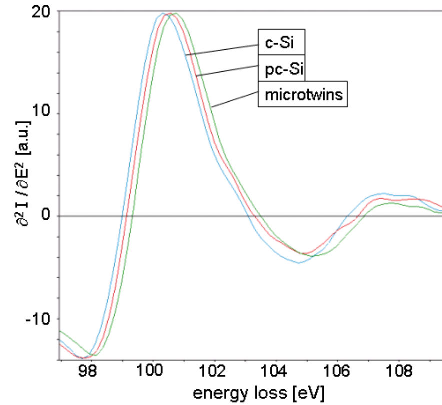

Figure 5: Second derivative of the Si-$L_{2,3}$ edges of an area with perfect crystallinity (*c-Si*), the polycrystalline defect (*pc-Si*) and the microtwins (*microtwins*). The threshold energies are shifted by +0.2eV and +0.3eV for the *pc-Si* and the *microtwins*, respectively.

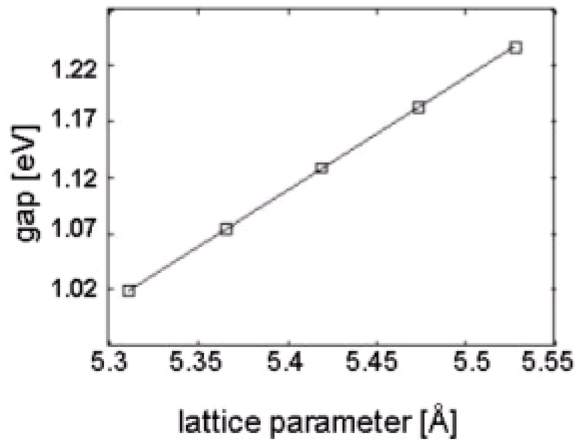

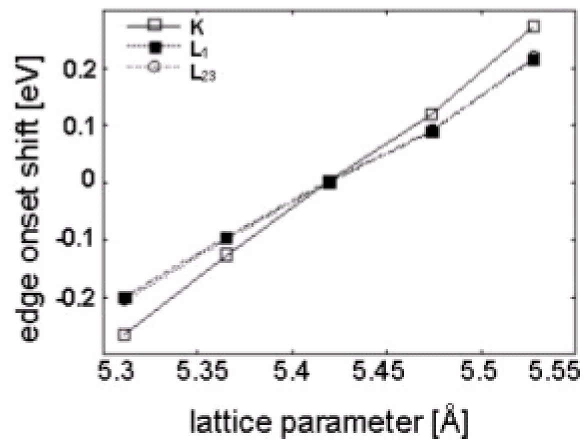

Figure 6: Gap width (in eV) vs. varying lattice parameter (±2%) on the left side. The lattice parameter of c-Si is 5.429Å. Energy shift of the ionisation edge vs. lattice parameter for the Si $L_{2,3}$, L_1, and K edges on the right side.

ACKNOWLEDGEMENTS

The University Service Centre for Transmission Electron Microscopy (USTEM) of the Vienna University of Technology is kindly acknowledged for giving access to its TECNAI F20 ST.

REFERENCES

Blaha P, Schwarz KH, Madsen G, Kvasnicka D and Luitz J 2002 ISBN 3-9501031-1-2
Citrin PH, Wertheim GK and Baer Y 1978 Phys. Rev. Lett. **41**, 1425
Citrin PH and Wertheim GK 1983 Phys. Rev. B **27**, 3176
Eastman DE, Himpsel FJ and van der Veen JF 1982 Vac. Sci. Technol. **20**, 609
Mizushima I, Koike M, Stao T, Miyano K and Tsunashima Y 1999 Jpn. J. Appl. Phys. **38**, 2415
Muller D 1999 Ultramicroscopy **78**, 163
Platen J, Selle B, Sieber I, Brehme S, Zeimer U and Fuhs W 2001 Thin Sol. Film. **381**, 22
Steiner P and Hüfner S 1981 Acta Metall. **29**, 1885